Progress In Electromagnetics Research Letters, Vol. 105, 131–137, 2022

A Flexible, Foldable Metamaterial Absorber Fabricated by Matrix-Assisted Catalytic Printing

Pengyu Gong[1, 2, †], Huan Lu[1, 3, *, †], Bo Yang[4], Ruisheng Guo[5], Siqi Zhang[1], and Rongrong Zhu[1, 2, *]

Abstract—Metamaterial absorbers are widely used in sensing, clocking, imaging, etc. Currently, most metamaterial absorbers are integrated by hard substrates, which limit their applications for non-planar and irregular surfaces. In this paper, a flexible, foldable metamaterial absorber is proposed using a matrix-assisted catalytic printing method. The absorber is composed of periodically patterned eight-round sector copper arrays supported by a polyethylene terephthalate substrate. Experimental results show that the absorber exhibits one absorption peak near 10.2 GHz.

1. INTRODUCTION

Metamaterials are artificial materials formed by periodic "meta-atoms" to exhibit unique electromagnetic properties that are not available in natural materials [1, 2]. Due to their exceptional properties, massive researches on metamaterials have been carried out in recent years. Numerous related applications have been proposed [3–16], such as invisibility cloaks, super-diffusers, spinners sensors, optical illusion devices, and absorbers. Among these applications, metamaterial absorbers (MAs) attracted significant research interests because of their high absorption capability. Since Landy et al.'s pioneering work in 2008 [16], various MAs have been proposed [17–26], playing important roles in various fields including sensing, cloaking, imaging, etc.

However, many studies of MAs have focused on the use of hard substrates. These MAs are not flexible enough that are not able to conformally overlay complex, irregular surfaces. Although there are also MAs using special materials such as ITO (Indium Tin Oxide) as substrates that are ultrathin and flexible, these MAs are limited to specific materials and not able to be folded.

In this paper, we propose one MA achieved by matrix-assisted catalytic printing (MACP) technology [27]. As a demonstration, we use polyethylene terephthalate (PET) as the substrate and patterned copper on PET to make the metal resonant unit cell. Experimental results show that the absorber exhibits one absorption peak near 10.2 GHz. This absorber is flexible and foldable made by MACP process and could conformally overlay on complex, irregular surfaces. Owing to these properties, it is expected that this proposed MA may have great potential for non-planar and conformal applications.

Received 4 July 2022, Accepted 21 July 2022, Scheduled 4 August 2022

* Corresponding author: Rongrong Zhu (rorozhu@zju.edu.cn), Huan Lu (luhuan123@zju.edu.cn). † These authors contributed equally to this work.

[1] Interdisciplinary Center for Quantum Information, State Key Laboratory of Modern Optical Instrumentation, ZJU-Hangzhou Global Scientific and Technological Innovation Center, Zhejiang University, Hangzhou 310027, China. [2] School of Information and Electrical Engineering, Zhejiang University City College, Zhejiang 310015, China. [3] International Joint Innovation Center, Key Lab. of Advanced Micro/Nano Electronic Devices & Smart Systems of Zhejiang, The Electromagnetics Academy at Zhejiang University, Haining, Zhejiang 314400, China. [4] Sussex Artificial Intelligence Institute, Zhejiang Gongshang University, Zhejiang 310018, China. [5] State Key Laboratory of Solidification Processing, Center of Advanced Lubrication and Seal Materials, School of Materials Science and Engineering, Northwestern Polytechnical University, Xi'an, Shanxi 710072, China.

2. DESIGN AND SIMULATION RESULTS

Figure 1(a) presents a schematic illustration of the proposed MA. The unit cell and some relevant parameters are shown in Figs. 1(b) and (c). It consists of three layers: a metal resonant structure, a dielectric substrate, and a metal backplane. Its simulation focuses on the metal resonant structure and dielectric substrate. The PET is used to design the flexible dielectric substrate. The dielectric constant of high purity undoped glass fiber PET is $3.1(1 + i0.025)$, and the tangent of the dielectric loss angle is 0.008. The material used for the metal resonant structure is copper with a conductivity of $\sigma = 5.8 \times 10^7$ S/m and a thickness of 0.5 μm.

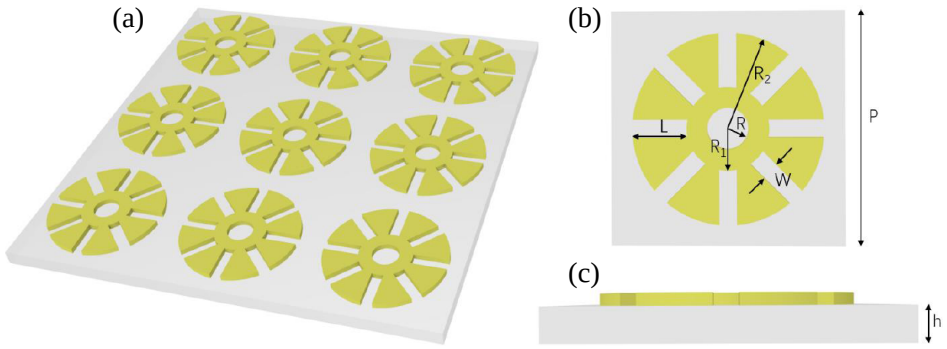

Figure 1. Schematic of the proposed MA. (a) Perspective view of the proposed MA. (b) Top view of the unit cell. $P = 7$ mm, $R = 0.7$ mm, $R_1 = 1.4$ mm, $R_2 = 3.25$ mm, $W = 0.6$ mm. (c) Side view of the unit cell. $h = 0.25$ mm.

The overall unit cell is an eight-round sector (ECS) structure, with a circular structure in the middle. There are mainly five design parameters: P, W, R, R_1, and R_2. P refers to the overall length of the unit cell (including the distance from the left and right unit structures); W refers to the width of the gap between each sector; R is the radius of the hollow circle in the center; R_1 and $R_2(R = R_1 + L)$ are the radii of the inner and outer circles, respectively, and L is the side length of the sector. Since the proposed MA is fully symmetric, the absorption efficiency of the MA is insensitive to the polarization angle at normal incidence.

The absorption A could be defined as $A = 1-|S_{11}|^2-|S_{21}|^2$, where S_{11} is the coefficient of reflection, and S_{21} is the coefficient of transmission. Since the thickness of the metal ground plane is much larger than the penetration depth of electromagnetic waves, S_{21} is considered as zero, and the absorption could be simplified as $A = 1 - |S_{11}|^2$. The absorption spectrum of the simulation result is shown in Fig. 2(a). The simulation result exhibits one absorption peak at 10.2 GHz. The basic principles of MAs can be

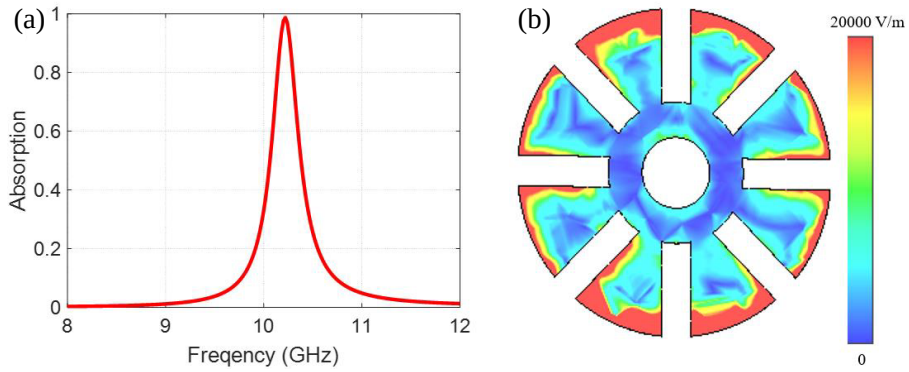

Figure 2. Simulation results. (a) Simulated absorption spectrum of proposed MA. (b) Electric field distribution in ECS structure.

explained from electrical and magnetic resonance perspective, which can be visualized by plotting the electric field magnitude. Fig. 2(b) shows the electric field distribution in ECS structure. It is observed that the electric field is strongly coupled to the ECS structure. Under the effect of the electric field, a large number of electric charges are accumulated at the arcs of the ECS structure, causing a strong electrical response. Perfect absorption is caused by the LC resonance in the ECS structure.

3. FABRICATION

The MACP method is used in the fabrication process. MACP is a multi-functional printing method for low-cost and simple fabrication of metal conductors on various flexible materials such as plastic and textile substrates. With the help of MACP, we are able to fabricate metal conductors with multi-scale and complex patterns on various plastic and flexible material substrates.

In MACP method, catalytic salt is printed, with the help of a delivering matrix polymer, onto a substrate with a thin layer of receiving matrix polymer [28–30]. In the fabrication process, we choose polyethylene glycol (PEG), poly[2-(methacryloyloxy)ethyl-trimethylammonium chloride] (PMTEAC), and $(NH_4)_2PdCl_4$ as the catalyst salt, delivering matrix polymer, receiving matrix polymer, and catalyst salt, respectively.

The overall fabrication procedure is shown in Fig. 3. The first step of the whole procedure is surface treatment which has a great impact on subsequent metal pattern printing. The PET was immersed in an ethanol solution containing Vinyltriacetoxy-silane (VTMS) to make it able to bond the polymer brush layer tightly. Then, the PET was soaked in deionized water containing Methacryloxyethyltrimethyl ammonium chloride (METAC) and Potassium persulfate (KPS). The purpose of this step is to form a layer of PMETAC polymer brush on the surface, which facilitates the subsequent adhesion of the catalysts. Then the PET was cleaned and dried. The next step is screen-printing catalytic ink. The ink used in screen-printing is composed of PEG and $(NH_4)_2PdCl_4$. In screen-printing process, the catalysts diffused through the screen and formed ink pattern on the surface of the PET substrate. Thus, the PET dielectric substrate with a catalyst layer bound on the surface can be obtained. The last step is electroless deposition in the presence of catalysts. The PET was put in a specially formulated solution (sodium hydroxide, copper sulfate pentahydrate, sodium tartrate and formaldehyde) to deposit copper pattern by electroless deposition. The as-fabricated copper pattern on PET was MA.

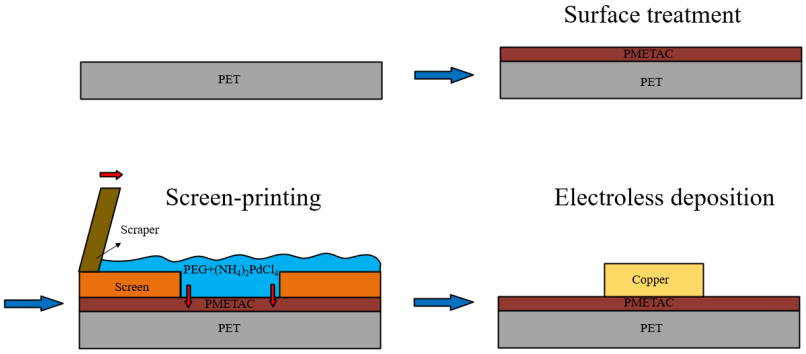

Figure 3. Schematic illustration of the fabrication process. Surface treatment could form a layer of PMETAC on the PET. Screen-printing could print the catalyst ($(NH_4)_2PdCl_4$) as we want. Finally, the copper deposits on the catalyst region thus form the metal pattern.

4. EXPERIMENTAL RESULTS

Several samples were fabricated with the aid of the MACP. The high-transparent flexible substrate PET used in fabrication maintains its light-transmitting characteristics before and after fabrication, and the metal pattern printed on the surface maintains its own shape well in the process of bending, deformation, and friction, without breaking and damage, showing great flexibility and foldability.

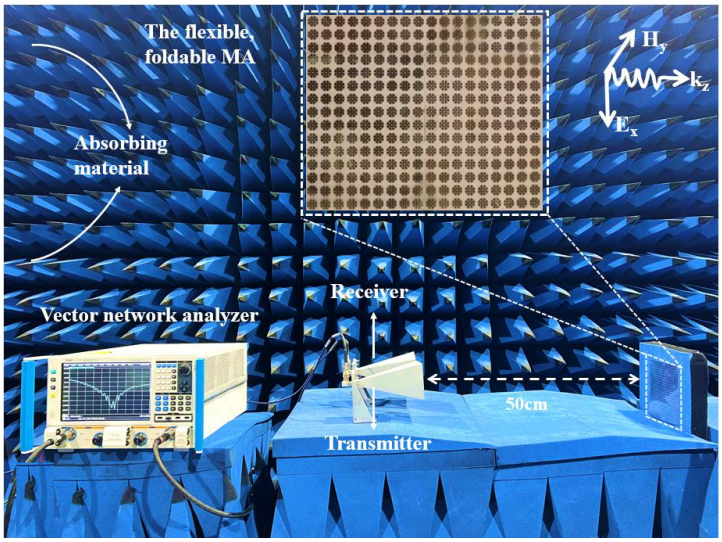

Figure 4. Measurement setup for evaluating the performance of the MA. The metasurface is placed in an anechoic chamber. The transmitter and the probe are connected to the vector network analyzer. The transmitter is set at approximately 50 cm away from the MA. The inset shows a schematic of the details of the sample.

The reflection of the samples was measured by a pair of horn antennas connected to a Ceyear 3672A vector network analyzer. Measurement setup is shown in Fig. 4. The reflection of a copper plate with the same size at the same position was also measured as a comparison. Fig. 5(a) shows the absorption spectrums of the experiment results. We observe that the samples can achieve high absorption at 10, 10.3, 107, and 11.2 GHz, respectively. Compared with the simulation results, the frequency of absorption peak is not the same, and the absorption frequency band expands to a certain extent.

There are some differences between the performance of the MA obtained by the experimental tests and the simulation. The causes are as follows: due to the pattern diffusion caused by ink leakage, screen printing will lead to the increase of R_1, R_2 and the decrease of W, R, thus the frequency of the absorption peak will become higher, as shown in Fig. 5(b); because of the limitation of the size of the container, the immersion in the substrate fabrication process is not sufficient, resulting in a loose combination of some catalysts and the dielectric substrate, so that the substrate cannot deposit enough

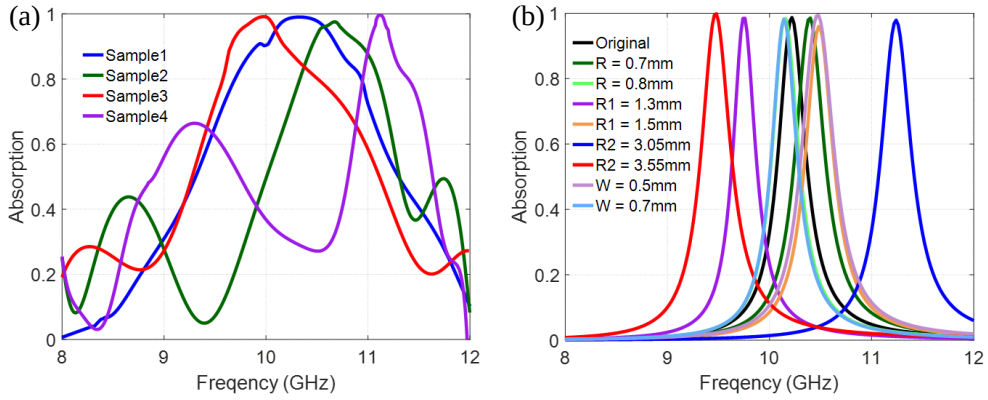

Figure 5. (a) Absorption spectrums of the experiment results. (b) Absorption spectrums of the MA for different structural parameters. The black curve represents the original simulation result, whereas curves of other colors represent simulation results of different parameters.

metal, and R_1, R_2 decrease while W, R increase, thus the frequency of the absorption peak will become lower, as shown in Fig. 5(b); metallic copper will be gradually oxidized after deposition, which will affect the absorption performance.

Because of the above reasons, the fabricated sample is actually equivalent to a metasurface composited with multiple similar structures with different parameters, and the overall absorption frequency band is equivalent to a composite of multiple frequency bands. The overall performance of the sample will change owing to the change of the unit structure. Therefore, there is a certain deviation from the simulation results.

5. CONCLUSION

In summary, an MA achieved by MACP has been proposed. The absorber is composed of a periodically patterned eight-round sector copper arrays supported by a PET substrate. The procedure of the fabrication based on MACP is introduced. Several samples were fabricated by MACP successfully. The performance of the MA is demonstrated with simulation and experimental test. The experimental results exhibit one absorption peak near 10.2 GHz. The proposed MA is flexible, foldable, and able to conformally overlay complex, irregular surfaces, which can be used in non-planar and conformal applications.

ACKNOWLEDGMENT

Natural Science Foundation of Zhejiang Province (No. LQ21F050002).

DISCLOSURES

The authors declare no competing financial interest.

DATA AVAILABILITY

Data underlying the results presented in this paper are not publicly available at this time but may be obtained from the authors upon reasonable request.

REFERENCES

1. Veselago, V. G., "The electrodynamics of substances with simultaneously negative values of ε and μ," *Physics-Uspekhi*, Vol. 10, No. 4, 509–514, 1968.
2. Shamonina, E. and L. Solymar, "Metamaterials: How the subject started," *Metamaterials*, Vol. 1, 12–18, 2007.
3. Schurig, D., J. J. Mock, B. J. Justice, S. A. Cummer, J. B. Pendry, A. F. Starr, and D. R. Smith, "Metamaterial electromagnetic cloak at microwave frequencies," *Science*, Vol. 314, No. 5801, 977–980, 2006.
4. Gao, X., W. L. Yang, H. Ma, Q. Cheng, X. Yu, and T. Cui, "A reconfigurable broadband polarization converter based on an active metasurface," *IEEE Transactions on Antennas and Propagation*, Vol. 66, No. 11, 6086–6095, 2018.
5. Tian, X., P. Lee, Y. Tan, T. Wu, H. Yao, M. Zhang, and J. Ho, "Wireless body sensor networks based on metamaterial textiles," *Nature Electronics*, Vol. 2, No. 6, 243–251, 2019.
6. Cai, T., S. Tang, B. Zheng, G. Wang, W. Ji, C. Qian, and H. Chen, "Ultrawideband chromatic aberration-free meta-mirrors," *Advanced Photonics*, Vol. 3, No. 1, 016001, 2020.
7. Beruete, M. and I. Jáuregui-López, "Terahertz sensing based on metasurfaces," *Advanced Optical Materials*, Vol. 8, No. 3, 1900721, 2020.

8. Lu, H., B. Zheng, C. Qian, Z. Wang, Y. Yang, and H. Chen, "Frequency-controlled focusing using achromatic metasurface" *Advanced Optical Materials*, Vol. 9, No. 1, 2001311, 2021.
9. Zhang, J., X. Wei, I. D. Rukhlenko, H. T. Chen, and W. Zhu, "Electrically tunable metasurface with independent frequency and amplitude modulations," *ACS Photonics*, Vol. 7, No. 1, 265–271, 2019.
10. Tan, Q., B. Zheng, T. Cai, C. Qian, R. Zhu, X. Li, and H. Chen, "Broadband spin-locked metasurface retroreflector," *Advanced Science*, 2201397, 2022.
11. Yao, H., H. Mei, W. Zhang, S. Zhong, and X. Wang, "Theoretical and experimental research on terahertz metamaterial sensor with flexible substrate," *IEEE Photonics Journal*, Vol. 14, No. 1, 1–9, 2021.
12. Huang, M., B. Zheng, T. Cai, X. Li, J. Liu, C. Qian, and H. Chen, "Machine-learning-enabled metasurface for direction of arrival estimation," *Nanophotonics*, Vol. 11, No. 9, 2001–2010, 2022.
13. He, Q., S. Sun, S. Xiao, and L. Zhou, "High-efficiency metasurfaces: Principles, realizations, and applications," *Advanced Optical Materials*, Vol. 6, 1800415, 2018.
14. Ding, F., A. Pors, and S. I. Bozhevolnyi, "Gradient metasurfaces: A review of fundamentals and applications," *Reports on Progress in Physics*, Vol. 81, 026401, 2018.
15. Di Renzo, M., A. Zappone, M. Debbah, M. S. Alouini, C. Yuen, J. De Rosny, and S. Tretyakov, "Smart radio environments empowered by reconfigurable intelligent surfaces: How it works, state of research, and the road ahead," *IEEE Journal on Selected Areas in Communications*, Vol. 38, No. 11, 2450–2525, 2020.
16. Landy, N. I., S. Sajuyigbe, J. J. Mock, D. R. Smith, and J. Padilla, "Perfect metamaterial absorber," *Physical Review Letters*, Vol. 100, 207402, 2008.
17. Tao, H., N. I. Landy, C. M. Bingham, X. Zhang, R. D. Averitt, and W. J. Padilla, "A metamaterial absorber for the terahertz regime: Design, fabrication and characterization," *Optics Express*, Vol. 16, 7181–7188, 2008.
18. Sun, P., C. You, A. Mahigir, T. Liu, F. Xia, W. Kong, and M. Yun, "Graphene-based dual-band independently tunable infrared absorber," *Nanoscale*, Vol. 10, No. 33, 15564–15570, 2018.
19. Zhao, X., Y. Wang, J. Schalch, G. Duan, K. Cremin, and J. Zhang, "Optically modulated ultra-broadband all-silicon metamaterial terahertz absorbers," *ACS Photonics*, Vol. 6, No. 4, 830–837, 2019.
20. Zou, H. and Y. Cheng, "Design of a six-band terahertz metamaterial absorber for temperature sensing application," *Optical Materials*, Vol. 88, 674–679, 2019.
21. Xiong, H., Q. T. Ji, Bashir, and F. Yang, "Dual-controlled broadband terahertz absorber based on graphene and dirac semimetal," *Optics Express*, Vol. 28, No. 9, 13884–13894, 2020.
22. Verma, V. K., S. K. Mishra, K. K. Kaushal, N. Gupta, and B. Appasani, "An octaband polarization insensitive terahertz metamaterial absorber using orthogonal elliptical ring resonators," *Plasmonics*, Vol. 15, No. 1, 75–81, 2020.
23. Lin, K. T., H. Lin, T. Yang, and B. Jia, "Structured graphene metamaterial selective absorbers for high efficiency and omnidirectional solar thermal energy conversion," *Nature Communications*, Vol. 11, No. 1, 1389, 2020.
24. Qi, L. and C. Liu, "Broadband multilayer graphene metamaterial absorbers," *Optical Materials Express*, Vol. 9, No. 3, 1298–1309, 2019.
25. Feng, H., Z. Xu, L. I. Kai, M. Wang, and M. Yun, "Tunable polarization-independent and angle-insensitive broadband terahertz absorber with graphene metamaterials," *Optics Express*, Vol. 29, No. 5, 7158–7167, 2021.
26. Yao, Y., Z. Liao, Z. Liu, X. Liu, J. Zhou, G. Liu, and J. Wang, "Recent progresses on metamaterials for optical absorption and sensing: A review," *Journal of Physics D: Applied Physics*, Vol. 54, No. 11, 113002, 2021.
27. Guo, R., Y. Yu, Z. Xie, X. Liu, X. Zhou, and Y. Gao, "Matrix-assisted catalytic printing for the fabrication of multiscale, flexible, foldable, and stretchable metal conductors," *Advanced Materials*, Vol. 25, No. 24, 3343–3350, 2013.

28. Azzaroni, O., Z. Zheng, Z. Yang, and W. Huck, "Polyelectrolyte brushes as efficient ultrathin platforms for site-selective copper electroless deposition," *Langmuir the Acs Journal of Surfaces & Colloids*, Vol. 22, No. 16, 6730–6733, 2006.
29. Liu, X., H. Chang, Y. Li, W. T. Huck, and Z. Zheng, "Polyelectrolyte-bridged metal/cotton hierarchical structures for highly durable conductive yarns," *ACS Applied Materials & Interfaces*, Vol. 2, No. 2, 529–535, 2010.
30. Wang, X., H. Hu, Y. Shen, X. Zhou, and Z. Zheng, "Stretchable conductors with ultrahigh tensile strain and stable metallic conductance enabled by prestrained polyelectrolyte nanoplatforms," *Advanced Materials*, Vol. 23, No. 27, 3090–3094, 2011.